

TW Hya Association Membership and New WISE-detected Circumstellar Disks

Adam Schneider

Department of Physics and Astronomy, University of Georgia, Athens, GA 30602

aschneid@physast.uga.edu

Carl Melis

Center for Astrophysics and Space Sciences, University of California, San Diego, CA 92093

cmelis@ucsd.edu

and

Inseok Song

Department of Physics and Astronomy, University of Georgia, Athens, GA 30602

song@physast.uga.edu

ABSTRACT

We assess the current membership of the nearby, young TW Hydrae Association and examine newly proposed members with the Wide-field Infrared Survey Explorer (WISE) to search for infrared excess indicative of circumstellar disks. Newly proposed members TWA 30A, TWA 30B, TWA 31, and TWA 32 all show excess emission at 12 and 22 μm providing clear evidence for substantial dusty circumstellar disks around these low-mass, ~ 8 Myr old stars that were previously shown to likely be accreting from circumstellar material. TWA 30B shows large amounts of self-extinction, likely due to an edge-on disk geometry. We also confirm previously reported circumstellar disks with WISE, and determine a 22 μm excess fraction of $42_{-9}^{+10}\%$ based on our results.

Subject headings: open clusters and associations: individual (TW Hydrae Association) brown dwarfs: - circumstellar matter - stars: evolution - stars: low-mass - stars: pre-main-sequence

1. Introduction

Young stars in the vicinity of the classical T-Tauri star TW Hydrae were first proposed to be associated by Kastner et al. (1997). Since then, many new members have been proposed and studied, and the TW Hydrae association (TWA) is now currently made up of a few dozen members (see Barrado Y Navascues 2006 and Torres et al. 2008 for the most recent membership reviews). TWA has an age of ~ 8 Myr, a critical age of stellar evolution and planet formation, between that of T-Tauri and main sequence stars. This association’s young age and proximity to the Sun (~ 50 pc) have made it an area of intense study, most notably for low-mass members (such as 2M1207b; Chauvin et al. 2004) and circumstellar disks (e.g. Weinberger et al. 2004, Low et al. 2005, Rebull et al. 2008, and Riaz & Gizis 2008).

Previous studies of dusty disks in TWA have shown a diverse array of disk properties for its members, spanning a range of evolutionary stages. The first four disks (TW Hya, Hen-3 600, HD 98800, and HR4796A) were detected with the *Infrared Astronomical Satellite* (IRAS). After the discovery of new members, surveys were performed to identify any additional sources with IR-excess above predicted stellar photospheres using mid-IR imaging from the ground (Weinberger et al. 2004) and space (Low et al. 2005) with the *Spitzer Space Telescope* (Werner et al. 2004). Until recently, no additional members showing strong IR-excess emission have been found, though some members showing small amounts of excess ($\tau \equiv L_{IR}/L_* < 0.5\%$) have been proposed (TWA 7 and TWA 13 - Low et al. 2005; TWA 8B and TWA 19 - Rebull et al. 2008). The surveys by Weinberger et al. (2004) and Low et al. (2005) show a clear bimodal distribution of excess emission at mid-IR wavelengths, indicating that most members have negligible amounts of warm dust surrounding them. Disks have since been discovered around 4 new TWA members not included in the previous mid-IR studies, 2M1207 (Sterzik et al. 2004), SSPM 1102 (Riaz & Gizis 2008 and Morrow 2008), TWA 30A (Looper et al. 2010a), and TWA 30B (Looper et al. 2010b). These four most recent disk discoveries are all around late-type members (spectral types $\geq M4$), indicating a very high disk fraction for objects of this type in TWA.

A new method of identifying young stars employed by Rodriguez et al. (2011) utilizing UV-excess measurements from the *Galaxy Evolution Explorer* (GALEX; Martin et al. 2005) led to the proposal of several new TWA candidates. Shkolnik et al. (2011), using GALEX in a similar way, independently confirm the membership of one of the proposed candidates of Rodriguez et al. (2011) (TWA 32) and propose another additional member (TWA 31).

With the *Wide-Field Infrared Explorer* (WISE), we now have the opportunity to explore each current member, old and new, with mid-IR wavelengths to search for excess emission indicative of circumstellar material. In this letter, we summarize assessment of TWA membership, and attempt to re-analyze all previous reports of IR-excess. We also evaluate all

members for which mid-IR photometry has not been performed, including new members, to search for evidence of any surrounding dusty disk.

2. Current Membership of TWA

Establishing the membership status of TWA is difficult. This is partly due to the overlap with the Lower-Centaurus Crux (LCC) region of the Scorpius Centaurus complex (Sco-Cen). Young stars found in this area can be difficult to place because the age of the LCC ($\sim 10\text{-}20$ Myr) is similar enough to that of TWA that youth indicators alone cannot distinguish between the two. Typically, a distance measurement is relied upon to make the final distinction, because the LCC is generally further away than TWA (LCC ~ 120 pc; TWA ~ 50 pc). However, with the addition of new members, such as TWA 29 ($d \sim 90$ pc) and TWA 31 ($d \sim 110$ pc), the boundary between the LCC and TWA is becoming much more ambiguous, providing evidence that TWA may indeed be the front edge of the LCC, as proposed by Song et al. (2003). For the purposes of this work, we choose a distance cut of 100 pc for the identification of TWA members, acknowledging that this choice will need further revision if more members are identified at intermediate distances.

A current summary of the properties of proposed TWA members is given in Table 1. When more than one value for a property of a particular object is available, we opt for the most recent measurement. A complete list of members is crucial when evaluating properties such as excess fractions, age, and group velocities. Torres et al. (2008) evaluated the membership of all proposed TWA members up to TWA designation 28 (including eight objects labeled as secondaries to TWA members), with the exception of 4 possible members for which kinematical data was found to be lacking. By applying a convergence method to the remaining 32 stars, 6 were found to have a TWA membership probability of zero (15A, 17, 18, 19A, 19B, and 24), and we agree with this assessment based on the discrepant distances found for these stars ($d > 100$) compared to those of members found to have a high probability of membership ($70 > d > 25$). Of the remaining, 2 stars were categorized as unlikely members (12 and 21), and 2 as possible members (6 and 14). A total of 22 stars were found to be high probability members.

TWA 15B, TWA 22, TWA 23, and TWA 28 were the four possible members not evaluated by Torres et al. (2008). As of this writing, TWA 15B still lacks the kinematical information necessary to properly evaluate its membership, though its estimated distance (100 pc) from Shkolnik et al. (2011), inconsistent with known TWA members, leads us to label its status as questionable. Teixeira et al. (2009) performed a thorough analysis of the kinematics of TWA 22, but the results were somewhat inconclusive. We retain TWA 22

as a possible member. Shkolnik et al. (2011) reevaluate the kinematics of TWA 23 (found to be spectroscopic binary), and show its UVW space motion is consistent with being a TWA member. In a similar fashion as TWA 22, Teixeira et al. (2008) thoroughly evaluate the membership of TWA 28 with high precision proper motion and parallax measurements, and determine it is a true member of TWA.

Since the review of Torres et al. (2008), six objects have been assigned TWA designations (11C, 29, 30A, 30B, 31, and 32). TWA 11C was discovered and determined to be a member of TWA by Kastner et al. (2008) via its common proper motion to TWA 11AB and strong lithium absorption and H α emission confirming its youth. For TWA 29, first proposed by Looper et al. (2007), we determine new proper motion values based on its 2MASS and WISE positions. These new values, listed in Table 1, along with its estimated distance, strong H α emission, and position relative to other TWA members, make its membership highly likely. TWA 30A and TWA 30B have been determined to be highly likely members by Looper et al. (2010a) and Looper et al. (2010b) respectively, and we agree with their analysis. Shkolnik et al. (2011) show that proposed members TWA 31 and 32 share spectroscopic, photometric, and kinematic properties with known members, thereby solidifying their membership. This is definitely the case for TWA 32, with UVW space motions¹ consistent with known TWA members. For TWA 31, though, this is not so obvious.

Shkolnik et al. (2011) quote a photometric distance to TWA 31 of 110 pc, a distance inconsistent with that of known members. Additionally, in their analysis, they compare the UVW of TWA 31 to some stars with questionable membership, such as TWA 12, 14, and 22, making the UVW for TWA 31 seem more reasonable than it should. The claim that TWA 31 is certainly too young to be an LCC member is valid when the LCC is assigned an age of 16 Myr. However, if the LCC is younger (~ 10 Myr, as suggested by Song et al. (2012)), then the use of age indicators as a deciding factor for membership in TWA or the LCC is unsound. As mentioned above, this may be one of many possible objects between TWA and the LCC that make a distinct boundary between the two unclear. We retain TWA 31 as a possible member for this study because of the large uncertainty ($\sim 10\%$) in its distance estimate.

In summary, of all stars with TWA designations, we find there to be 30 bona-fide TWA members, 4 possible members, one questionable member, 2 unlikely members, and 7 nonmembers. This is displayed in Table 1 with the following symbols representing the various designations: Y = true member, Y? = possible member, ? = questionable member,

¹UVW are defined with respect to the Sun. U is positive toward the Galactic center, V is positive in the direction of Galactic rotation, and W is positive toward the north Galactic pole.

N? unlikely member, and N = nonmember.

3. IR-Excess with WISE

For every confirmed member of TWA, we cross-correlate with the WISE catalog. Out of the 30 confirmed members of TWA, 26 were detected with WISE. The four not included in WISE (TWA 3B, TWA 4B, TWA 5B, and TWA 11B), all companions, are too close to their primary members to be resolved individually. Three members were too faint to be detected in WISE channel 4, only having upper limits (TWA 9B, TWA 26, and TWA 29). For these members, we searched the Spitzer Heritage Archive for possible detections at $24\ \mu\text{m}$ with the Multiband-Imaging Photometer for Spitzer (MIPS; Rieke et al. 2004) to contribute to our mid-IR excess statistics. TWA 26 was the only observed member able to be detected. Source extraction was performed on the MIPS Post Basic Calibrated Data (pBCD) mosaic files using the Astronomical Point Source Extraction (APEX) package for this source, and the resulting flux measurement is included in Table 2.

For the remaining members, all were detected in all four WISE bands. Spectral energy distributions (SEDs) were generated using available catalog data from Tycho-2, 2MASS, and WISE. Stellar photosphere fluxes are predicted from our SED fitting technique (as described in Rhee et al. 2007). We convert the WISE magnitudes to fluxes using the conversion factors from Wright et al. (2010) for each source, then look for excess by examining each SED individually and checking the ratio of the WISE channel 4 flux versus the predicted photospheric flux at $22\ \mu\text{m}$. We flag potential excess sources as those having a WISE measurement greater than 5 times the WISE photometric uncertainty above our photospheric flux estimate at $22\ \mu\text{m}$. Predicted photospheric flux estimates, measured WISE fluxes, and significance of excess calculations for possible and true members of TWA are given in Table 2 for WISE channels 1, 3, and 4 (WISE channel 2 is not included because the spectral models in the WISE channel 2 region are affected by the fundamental CO bandhead at $4.7\ \mu\text{m}$ for later-type stars). The significance of excess evaluation only takes into account the WISE photometric uncertainties and not any uncertainty from the spectral fitting.

As seen in Table 2, we recover previous reports of excess indicative of a dusty disk for TWA 1, 3A, 4A, 7, 11A, 27, 28, 30A, and 30B. We also find strong excess around newly proposed members TWA 31 and 32. The presence of dust around TWA 30A was inferred by Looper et al. (2010a), and 30B was determined to have IR-excess indicative of a disk in Looper et al. (2010b) based on their near-IR spectra, and we show the shape of the mid-IR emission in the SEDs of each in Figure 1, along with the two new disk detections for TWA 31 and 32. As seen in the figure, the excess mid-infrared emission for TWA 30A,

31, and 32 are each fit with a single blackbody. Incomplete excess information at longer wavelengths precludes a more detailed model fit. From these simple blackbody fits we are able to provide an estimate of each disk’s characteristic temperature and absorbing area (given by the parameters ‘T_{dust}’ and ‘ τ ’, respectively) from the available data. These values are displayed in Figure 1. A color-color diagram showing the clear distinction between excess and non-excess stars is shown in Figure 2.

The SED for TWA 30B shows a drastically different shape than that of the other sources. We believe that this unusual SED is due to the disk inclination. By using a spectral model for an M4 star scaled to the distance measured by Looper et al. (2010b) for TWA 30B, (dashed line in Figure 1), we see that the photospheric emission is obscured at least up to WISE channel 2. This object is likely obscured by an edge on disk, as suggested by Looper et al. (2010b). To fit the current data, we scale down the model spectrum to meet the J-band flux and fit the excess emission using two blackbodies of 660 and 190 K located at distances of 2 and 31 AU, respectively. The inner disk temperature is in good agreement with that found by ?. This is only one potentially viable model capable of fitting the currently available data. A more thorough analysis of this source across many wavelengths needs to be carried out before a complete understanding can be obtained.

Rebull et al. (2008) reevaluated the work done by Low et al. (2005) to determine a 24 μm excess fraction of $30 \pm 11\%$ for TWA. The disk fraction for TWA was again estimated in Looper et al. (2010a), using the list of members from Mamajek (2005). They determine an overall disk fraction of $35_{-8}^{+11}\%$. Using our updated list of current members (29 total, 23 individually detected at 22 μm with WISE, and one (TWA 26) detected at 24 μm with Spitzer), and WISE photometry, we determine a mid-IR excess fraction of (10/24) $42_{-9}^{+10}\%$. Members not detected at 22 μm with WISE (or 24 μm with Spitzer) are not included in our excess statistics. Uncertainties are estimated following the method found in the appendix of Burgasser et al. (2003). If possible members are included, the excess fraction becomes (11/28) $39_{-8}^{+10}\%$. If we focus solely on substellar members (spectral type $> M6$), all three detected in WISE channel 4 show excess emission (though TWA 26 shows no excess at 24 μm). Comparing this with that of the stellar members (7/23) $30_{-7}^{+11}\%$, we see a possible indication of a difference in the disk decay lifetimes of stellar and substellar members of TWA. Though the sample size of substellar members is quite small, this would support the results from Scholz et al. (2007) of mass-dependent disk lifetimes.

Wyatt (2008) evaluates the protoplanetary disk fraction (based on near-IR excess) as a function of age for sun-like stars, and show that most sun-like stars have dispersed their disks by 6 Myr. To extend this work into the M-type star regime, we cross-correlate with WISE the proposed members for the β Pictoris association (~ 12 Myr) and η Cha cluster ($\sim 5-8$ Myr;

Luhman & Steeghs 2004) from Torres et al. (2008) in the same manner as above for TWA, focusing solely on stars with spectral types between M0 and M6 (at this time, there are not enough substellar members of these similarly aged associations to probe any further than M6). Using the same excess criteria as for TWA, we find that for the η Cha cluster, of the 12 M-type stars listed in Torres et al. (2008), 11 of which are individually detected with WISE, 5 show $22\ \mu\text{m}$ excess. For the β Pic association, we find only one marginal case of $22\ \mu\text{m}$ excess out of 20 M-type members, coming from known debris disk-bearing member AU Mic (Song et al. 2002b; Rhee et al. 2007). In this spectral type range, we find a protoplanetary disk fraction of (4/19) $21_{-6}^{+12}\%$ for TWA (5/20, or $25_{-7}^{+11}\%$, if possible members are included). These results show a dramatic drop-off of protoplanetary disk-fraction with age for M-stars, from $45_{-3}^{+15}\%$ to $21_{-6}^{+12}\%$ for η Cha and TWA, to no evidence for protoplanetary disks in the β Pic association. This implies that protoplanetary disk dissipation in M-stars is a rapid process (occurring in a time-scale as short as a few Myr) with disk dispersal occurring sometime between 8 and 12 Myr.

4. Conclusion

Gathering the most recent relevant data, we have reassessed the current membership status of the TW Hydrae association. We find that there are 30 bona fide members. Of these 30, 26 members were detected at $22\ \mu\text{m}$ with WISE. Using predicted stellar photosphere fluxes from SED fitting, we find 7 stellar and 3 substellar members to show clear signs of IR-excess indicative of a circumstellar disk. This is the first unambiguous evidence of disks found for newly proposed members TWA 30A, TWA 31 and TWA 32, and the first mid-IR analysis of the disk around TWA 30B. Our analysis shows a difference between the stellar and substellar disk fraction, evidence of mass-dependent disk lifetimes. We also note the dramatic drop-off of excess fraction in M0-M6 type stars when compared to the similarly aged η Cha cluster and the β Pic association.

This research has made use of the SIMBAD database and VizieR catalog access tool, operated at CDS, Strasbourg, France. This publication makes use of data products from the Two Micron All Sky Survey, which is a joint project of the University of Massachusetts and the Infrared Processing and Analysis Center/California Institute of Technology, funded by the National Aeronautics and Space Administration and the National Science Foundation, and the *Wide-field Infrared Survey Explorer*, which is a joint project of the University of California, Los Angeles, and the Jet Propulsion Laboratory/California Institute of Technology, funded by the National Aeronautics and Space Administration. We thank Adam J. Burgasser for a useful discussion. C. M. acknowledges support from the National Science

Foundation under award No. AST-1003318.

REFERENCES

- Barrado Y Navascues, D., 2006, *A&A*, 459, 511
- Burgasser, A. J., et al. 2003, *ApJ*, 586, 512
- Castro, P. J., Gizis, J. & Gagne, M. 2011, *ApJ*, 736, 67
- Chauvin, G., et al. 2004, *A&A*, 425, 29
- da Silva, L., et al. 2009, *A&A*, 508, 833
- de la Reza, R., & Pinzon G. 2004, *AJ*, 128, 1812
- Jayawardhana, R., Coffey, J., Scholz, A., Brandeker, A., & van Kerkwijk, M. 2006, *ApJ*, 648, 1206
- Kastner, J. H., Zuckerman, B., Weintraub, D., & Forveille, T. 1997, *Science*, 277, 67
- Kastner, J. H., Zuckerman, B., & Bessell, M. 2008, *A&A*, 491, 829
- Looper, D. L., Burgasser A., Kirkpatrick J., & Swift, B. 2007, *ApJ*, 669, L97
- Looper, D. L., et al. 2010a, *ApJ*, 714, 45
- Looper, D. L., et al. 2010b, *AJ*, 140, 1486
- Low, F., et al. 2005, *ApJ*, 631, 1170
- Luhman, K., & Steeghs, D. 2004, *ApJ*, 609, 917
- Mamajek, E., 2005, *ApJ*, 634, 1385
- Mathis, J. S., 1990, *ARA&A*, 28, 37
- Martin, D. C., et al. 2005, *ApJ*, 619, L1
- Mohanty, S., Jayawardhana, J. & Barrado Y Navascues, D. 2003, *ApJ*, 593, L109
- Morrow, A. L., 2008, *ApJ*, 676, L143
- Rebull, L. M., et al. 2008, *ApJ*, 681, 1484

- Reid, N., 2003, MNRAS, 342, 837
- Rhee, J. H., Song, I., Zuckerman, B., & McElwain, M. 2007, ApJ, 660, 1556
- Riaz, B., & Gizis, J. 2008, ApJ, 681, 1584
- Rieke, G. H., et al. 2004, ApJS, 154, 25
- Rodriguez, D. R., Bessell, M., Zuckerman, B., & Kastner, J. 2011, ApJ, 727, 62
- Shkolnik, E. L., Liu, M., Reid, I., Dupuy, T., & Weinberger, A. 2011, ApJ, 727, 6
- Scholz, A., et al. 2007, ApJ, 660, 1517
- Song, I., Weinberger, A., Becklin, E., Zuckerman, B., & Chen, C. 2002, ApJ, 124, 514
- Song, I., Zuckerman, B. & Bessell, M. 2003, ApJ, 599, 342
- Song, I., Zuckerman, B. & Bessell, M. 2012, arXiv1204.5715
- Sterzik, M. F., Pascucci, I., Apai, D., van der Blik, N., & Dullemond, C. 2004, A&A, 427, 245
- Teixeira, R., et al. 2008, A&A, 489, 825
- Teixeira, R., et al. 2009, A&A, 503, 281
- Torres, G., et al. 2003, AJ, 125, 825
- Torres, C., Quast, G., Melo, C., & Sterzik, M. 2008, Handbook of Star Forming Regions, Vol. II: The Southern Sky, ASP Monograph Publications, Vol. 5, ed. B. Reipurth (San Francisco, CA: ASP), 757
- Weinberger, A. J., Becklin, E., Zuckerman, B., & Song, I. 2004, AJ, 127, 2246
- Werner, M. W., et al. 2004, ApJS, 154, 1
- Wright, E. L., et al. 2010, AJ, 140, 1868
- Wyatt, M. C., 2008, ARA&A, 46, 339

Table 1. TWA Membership

TWA	SpT	dist [pc]	pmra mas/yr	pmde mas/yr	V_{rad} km/s	Li mÅ	H α Å	$\log(L_x/L_{bol})$	$v\sin i$ km/s	Member?	refs.
1	K6Ve	53	-66.8 \pm 1.6	-15.2 \pm 1.3	12.66 \pm 0.22	435	-172.5	-2.59	6	Y	11,11,7,4,13,6,5,13
2A	M2Ve	48	-91.6 \pm 1.8	-20.1 \pm 1.3	10.58 \pm 0.51	520	-1.72	-3.54	13	Y	11,17,7,17,17,17,5,13
2B	M2	43	N	4,5,-,-,-,-,-,-
3A	M4Ve	31	-109.3 \pm 8.7	0.8 \pm 8.9	9.52 \pm 0.86	510	-40.89	-3.33	12	Y	11,17,7,17,17,17,5,13
3B	M4Ve	31	9.89 \pm 0.62	540	-4.26	...	12	Y	11,17,-,17,17,17,-,13
4A	K5V	44	-91.7 \pm 1.5	-30.0 \pm 1.5	12.74 \pm 0.10	380	0	-3.43	9	Y	11,11,7,4,13,2,5,13
4B	K7,M1	47	5.73 \pm 0.14	335,540	0	-3.44	...	Y	4,5,-,4,4,2,5,-
5A	M2Ve	38	-85.4 \pm 3.6	-23.3 \pm 3.7	13.30 \pm 2.00	630	-6.37	-3.05	54	Y	11,17,7,17,17,17,5,13
5B	M8Ve	45	-86 \pm 8	-21 \pm 8	13.4	300	-5.1	-3.4	16	Y	11,11,9,1,13,1,16,13
6	K7	51	-57.0 \pm 2.1	-20.9 \pm 2.1	16.9	560	-3.4	-2.82	79.5	Y?	4,7,7,3,4,6,5,6
7	M2Ve	34	-122.3 \pm 2.3	-29.3 \pm 2.3	12.21 \pm 0.24	550	-5.39	-2.38	4	Y	11,17,7,17,17,17,5,13
8A	M3Ve	44	-99.3 \pm 9.0	-31.3 \pm 8.9	8.34 \pm 0.48	550	-5.04	-2.99	7	Y	11,17,7,17,17,17,2,13
8B	M5Ve	27	-95.3 \pm 10.0	-29.5 \pm 10.3	8.93 \pm 0.27	580	-6.21	...	11	Y	11,17,7,17,17,17,-,13
9A	K5Ve	68	-52.8 \pm 1.3	-20.2 \pm 1.8	9.46 \pm 0.38	470	-2.1	-3.09	11	Y	11,11,7,4,13,6,5,13
9B	M1Ve	68	-70.7 \pm 13.3	-6.6 \pm 15.8	11.3	480	-4.3	-2.28	8	Y	11,11,7,3,13,6,5,13
10	M2Ve	67	-72.6 \pm 12.2	-32.1 \pm 12.3	6.75 \pm 0.40	500	-5.46	-2.93	6	Y	11,17,7,17,17,17,5,13
11A	A0V	67	-53.3 \pm 1.3	-21.2 \pm 1.1	9.4 \pm 2.3	0	-5.91	...	152	Y	11,11,7,4,13,5,-,13
11B	M2Ve	67	9 \pm 1	550	-3.5	-3.22	12	Y	11,11,-,4,13,6,5,13
11C	M4.5	67	-49.6 \pm 3	-25.1 \pm 3	...	630	-6.66	Y	19,19,19,-,19,19,-,-
12	M2	63	-36.3 \pm 8.6	-1.6 \pm 8.9	13.12 \pm 1.59	530	-51.0	...	16.2	Y?	4,17,7,17,17,17,-,6
13A	M1Ve	55	-67.4 \pm 11.8	-17.0 \pm 11.8	12.57 \pm 0.50	580	-3.0	...	12	Y	11,11,7,4,13,6,-,13
13B	M1Ve	55	11.67 \pm 0.64	550	-3.0	...	12	Y	11,11, ,4,13,6,-,13
14	M0	113	-43.4 \pm 2.6	-7.0 \pm 2.4	15.83 \pm 2.00	590	-5.68	-3.15	43.1	N?	4,17,7,17,17,17,5,6
15A	M1.5	41	-100.0 \pm 33.0	-16.0 \pm 6.0	11.2	650	-8.8	-2.82	21.3	N	4,7,7,3,4,6,5,6
15B	M2	100	10.03 \pm 1.66	550	-9.64	...	32.3	?	4,17,-,17,17,17,-,7
16	M1Ve	65	-53.3 \pm 5.2	-19.0 \pm 5.2	9.01 \pm 0.42	380	-3.08	-3.43	11	Y	11,17,7,17,17,17,5,13
17	K5	163	-28.0 \pm 8.5	-11.1 \pm 8.5	4.6	490	-3.2	-3.23	49.7	N	4,7,7,3,4,6,5,6
18	M0.5	121	-29.0 \pm 5.2	-21.2 \pm 5.2	6.9	420	-3.3	-3.29	24.1	N	4,7,7,3,4,6,5,6
19A	G5	109	-33.6 \pm 0.9	8.5 \pm 0.9	11.5 \pm 3.8	190	0.57	-3.48	25	N	4,7,7,4,4,2,5,5
19B	K7	103	-35.6 \pm 4.8	-7.5 \pm 4.6	15.2	400	-2.2	-2.99	48.7	N	4,7,7,2,4,6,5,6
20	M3Ve	73	-52.0 \pm 5.0	-16.0 \pm 6.0	8.1 \pm 4	160	-3.1	-3.09	30	Y	11,11,7,2,13,6,5,13
21	M1	45	-65.3 \pm 2.4	13.7 \pm 1.0	17.5 \pm 0.8	290	0.0	-3.59	...	N?	5,7,7,3,3,3,5,-
22	M5	22	-175.8 \pm 0.8	-21.3 \pm 0.8	13.57 \pm 0.26	650	-10.48	...	9.7	Y?	6,17,12,17,17,17,-,17
23	M1	61	-68.0 \pm 4.0	-23.0 \pm 4.0	8.52 \pm 1.20	500	8.12	-2.94	14.8	Y	6,17,7,17,17,17,5,6

Table 1—Continued

TWA	SpT	dist [pc]	pmra mas/yr	pmde mas/yr	V_{rad} km/s	Li mÅ	H α Å	$\log(L_x/L_{bol})$	$v\sin i$ km/s	Member?	refs.
24	K3	107	-34.4 ± 2.8	-13.1 ± 1.7	11.9 ± 0.9	340	-0.3	-3.16	13.0	N	6,7,7,3,3,6,5,6
25	M1Ve	51	-75.0 ± 2.0	-26.9 ± 1.4	9.2 ± 2.1	555	-2.4	-2.95	13	Y	11,11,7,3,13,6,5,13
26	M8Ve	41	-93 ± 5	-31 ± 10	11.6 ± 2	500	-44.7	-4.8	25	Y	11,11,9,1,13,8,16,13
27	M8Ve	53	-63 ± 3	-23 ± 2	11.2 ± 2	500	-10.2	<-4.8	13	Y	11,11,9,1,13,8,16,13
28	M8.5	55.2	-67.2 ± 0.6	-14.0 ± 0.6	-64 ± 3	<-4.0	...	Y	10,10,10,-,-,9,16,-
29	M9.5	90	-89.4 ± 10	-20.9 ± 10	-15 ± 3	Y	9,20,9,-,-,9,-,-
30A	M5	42	-89.6 ± 1.3	-25.8 ± 1.3	12.3 ± 1.5	610	-6.8	-3.34	...	Y	14,14,14,14,14,14,14,-
30B	M4	44	-83 ± 9	-30 ± 9	12 ± 3	500	-7.4	Y	15,15,15,15,15,15,-,-
31	M4.2	110	-42 ± 6	-36 ± 3	10.47 ± 0.41	410	-114.8	Y?	17,17,17,17,17,17,-,-
32	M6.3	53	-62.2 ± 3.5	-24.7 ± 3.9	7.15 ± 0.26	600	-12.6	<-3.10	...	Y	17,17,17,17,17,17,18,-

The references in column 12 refer to columns 2, 3, 4 and 5, 6, 7, 8, 9, and 10, respectively.

References: (1) Mohanty et al. (2003); (2) Reid (2003); (3) Song et al. (2003); (4) Torres et al. (2003); (5) de la Reza & Pinzon (2004); (6) Jayawardhana et al. (2006); (7) Mamajek (2005); (8) Barrado Y Navascues (2006); (9) Looper et al. (2007); (10) Teixeira et al. (2008); (11) Torres et al. (2008) (12) Teixeira et al. (2009); (13) da Silva et al. (2009); (14) Looper et al. (2010a); (15) Looper et al. (2010b); (16) Castro et al. (2011); (17) Shkolnik et al. (2011); (18) Rodriguez et al. (2011); (19) Kastner et al. (2008); (20) This work.

Table 2. TWA Excess Measurements^a

TWA	Phot	W1 Meas	mJy Err	Ex	Phot	W3 Meas	mJy Err	Ex	Phot	W4 Meas	mJy Err	Ex
1	366.7	447.0	13.4	6.0	34.5	486.5	6.2	72.5	11.0	2070.0	30.3	68.0
2	710.9	685.4	23.6	-1.1	77.1	81.9	1.2	4.0	25.8	24.5	1.1	-1.2
3AB	778.5	708.5	24.4	-2.9	98.1	891.9	13.0	60.8	33.3	1693.4	21.7	76.5
4AB	1912.2	1976.6	109.7	0.6	179.8	1807.6	19.9	81.9	57.4	6994.6	64.1	108.2
5AB	710.9	674.7	23.2	-1.6	77.1	86.7	1.3	7.6	25.8	24.9	1.1	-0.8
6	216.2	224.2	4.9	1.6	21.5	25.9	0.4	9.9	7.1	6.4	0.8	-0.8
7	576.6	581.2	15.8	0.3	57.3	72.9	1.0	15.6	18.9	33.1	1.2	12.2
8A	359.4	350.8	9.2	-0.9	40.0	44.5	0.5	9.0	13.4	12.8	1.0	-0.6
8B	101.0	88.3	4.8	-2.6	12.4	13.4	0.5	2.0	4.2	2.9	0.8	-1.4
9A	259.7	265.7	6.8	0.8	24.8	29.7	0.5	9.8	8.2	9.1	1.0	0.9
9B	83.0	77.2	3.5	-1.7	9.8	9.5	0.4	-0.8	3.29	<3.8
10	184.9	180.4	3.8	-1.2	21.8	22.6	0.4	2.0	7.3	6.7	0.6	-1.0
11AB	1442.3	2028.2	112.6	5.2	123.9	278.4	3.8	40.4	36.2	2713.7	34.8	77.0
11C	107.6	93.8	1.9	-7.2	15.5	14.5	0.3	-3.3	5.4	6.3	0.6	1.5
12	210.9	187.2	3.9	-6.1	21.6	23.7	0.4	5.25	7.2	5.2	0.8	-2.5
13A	294.3	273.3	12.8	-1.64	31.1	33.9	0.8	3.5	10.3	13.3	1.6	1.9
13B	350.2	326.5	16.1	-1.47	37.0	35.4	0.8	-2.0	12.3	8.2	1.5	-2.7
16	212.7	206.0	4.3	-1.6	23.7	25.4	0.4	4.3	7.9	8.0	0.7	0.1
20	149.8	145.0	3.0	-1.6	17.7	18.5	0.3	2.7	6.0	6.6	0.6	1.0
22	327.1	311.0	6.5	-2.5	41.2	46.0	0.6	8.0	14.0	15.8	0.8	2.3
23	288.9	271.6	6.4	-2.7	34.1	34.5	0.5	0.8	11.5	10.7	0.8	-1.0
25	392.3	384.7	10.1	-0.8	41.4	44.6	0.7	4.5	13.8	12.3	0.8	-1.9
26 ^b	11.1	10.7	0.2	-2.0	1.7	1.8	0.1	0.9	0.58	0.59	0.01	0.1
27	7.1	7.4	0.2	1.5	0.9	5.2	0.1	34.0	0.3	5.1	0.6	8.2
28	9.0	8.3	0.2	-3.5	1.4	5.6	0.2	21.0	0.5	5.2	0.8	5.9
29	1.6	2.0	0.1	4.0	0.2	0.3	0.3	0.3	0.1	<1.9
30A	115.3	93.8	1.9	-11.3	14.1	47.0	0.7	47.0	4.8	72.4	1.8	37.6
30B ^c	132.4	3.7	0.1	-1287.0	18.1	36.5	0.6	30.7	6.29	78.4	1.9	37.9
31	6.0	6.2	0.1	1.0	0.8	3.3	0.1	20.3	0.3	6.1	0.7	8.2
32	53.5	46.6	1.0	-6.8	7.7	24.3	0.4	43.9	2.7	40.5	1.4	27.9

^aFor late type stars, the spectral models in the WISE channel 2 region are affected by the fundamental CO bandhead at 4.7 μm , so are not included here. No color correction has been applied to the WISE data.

^bThe measured and estimated fluxes for TWA 26 in the W4 columns correspond to its MIPS 24 μm measurement.

^cThe estimated flux values for TWA 30 are from the distance-scaled spectral model (see Figure 1 and the discussion Section 3).

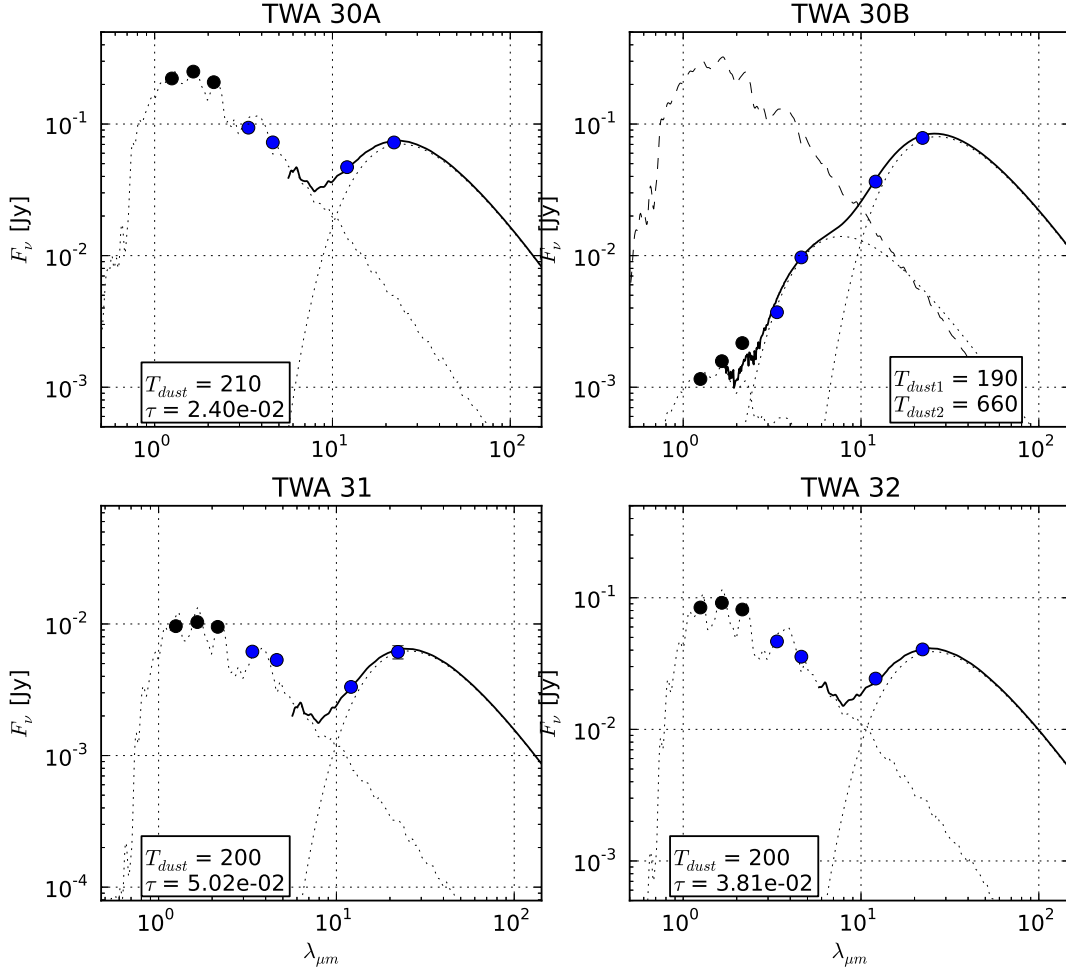


Fig. 1.— Spectral energy distributions (SED) for the four newest proposed members of TWA. The dotted curves are the spectral model and the single temperature blackbody dust fit. The solid curve is the spectral model + blackbody dust fit. For TWA 30B, the dashed line indicates the M4 model spectrum scaled to the distance quoted in Table 1 (see discussion in Section 3). The other curves represent the best fit to the currently available data as for TWA 30A, 31, and 32. To match the observed TWA 30B data points, we attempted to fit the SED with a combination of a reddened stellar spectrum using the standard ISM extinction relation (Mathis 1990) and gray extinction, but could not find a suitable fit. This implies that the dust grain size distribution around TWA 30B is different from that of ISM grains.

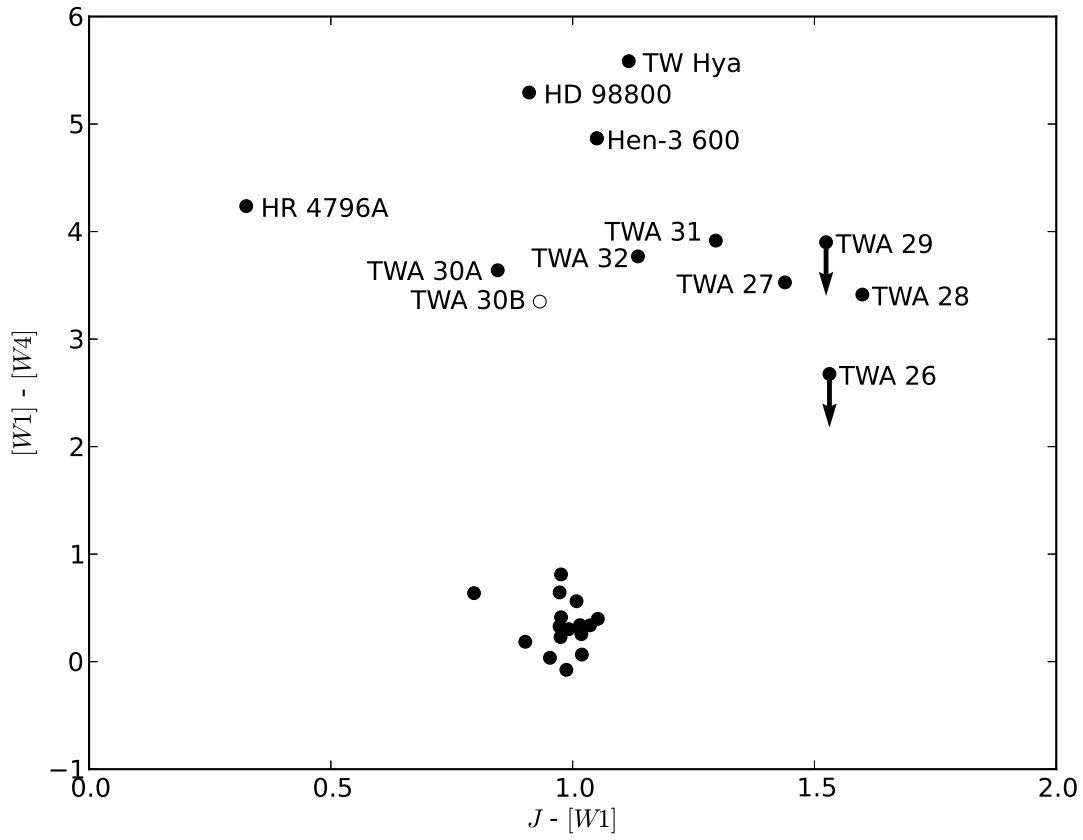


Fig. 2.— J - $W1$ vs. $W1$ - $W4$ color-color diagram for all individually detected TWA true and possible members. A clear distinction can be seen between those sources harboring disks and those without. For TWA 30B (open symbol), the J and $W1$ magnitudes are determined from the spectral model, while $W4$ is the measured magnitude. The actual position of TWA 30B on this figure from its measured data is $[2.2, 7.2]$.